

# Gate All Around FET: An Alternative of FinFET for Future Technology Nodes

Chander Mohan<sup>1</sup>, Sumit Choudhary<sup>2</sup>, B. Prasad<sup>3</sup>

<sup>1,2,3</sup>Department of Electronic Science, Kurukshetra University, Kurukshetra, Haryana, (India)

## ABSTRACT

Scaling of devices is reaching a brick wall because of short channel effects and quantum behavior of carriers at this scaled level. At this level, the quantum mechanics became more commanding over classical mechanics. To keep Moore's law alive, Gate All Around FET is a better candidate over FinFET and other existing sub 22 nm device architectures because of its gate coupling which tunes the channel more precisely and accurately. In GAA device architecture the SCE are minimized as compared to FinFET at same technology node. Physical device models of quantum level and their calibrated parameters used to simulate devices below 14nm technology were discussed. In this paper the transfer characteristics, output characteristics, gain, mobility roll off, subthreshold slope,  $I_{ON}/I_{OFF}$  ratio and DIBL of GAAFET simulated. Also compared these SCE in squared channel GAA and Cylindrical Channel GAA Structures. Simulated result shows that the SCEs were significantly reduced in cylindrical GAAFET. DIBL and SS were found to be 78mV/dec and 71mV/V vs. 113mV/dec and 73mV/V in Cylindrical GAAFET, Square channel GAAFET respectively.

**Keywords:** ATLAS, FinFET, Gate All Around (GAA), Scaling, Short Channel Effects (SCEs).

## I. INTRODUCTION

From past half century, Transistor is being continuously proven to be the most significant invention of engineering and is the backbone of every field. The secret to this much success lies in the fact that Transistor has followed a constant miniaturization trend initially predicted by G. Moore [1]. While it was a standard to have a feature size of 10  $\mu$ m in early days of MOSFET development [2], now the same is nearly 10 nm, and efforts are continuously made to shrink it more. This trend has allowed semiconductor industry to provide more and more features with reduced cost and power consumption. But, scaling has its own limitations, which further became more significant and challenging to rectify for feature size in Nanometer regime [3]. Device with feature sizes below 100 nm range suffers from lateral SCEs such as dopant fluctuation, hot electron effect, carrier velocity saturation, drain induced barrier lowering (DIBL). Subthreshold Swing (SS), leakage current, etc. and vertical gate insulator tunneling [4] [5] [6] [7].

Due to fundamental physical limitations, the scaling of planer MOSFET was predicted to be limited to 15nm, but it has already ended with 32nm technology node due to difficulties in maintaining the gate coupling of device with planer structure. To minimise SCEs and to improve the device performance changes such as strained Silicon, Silicon on Insulator (SOI), high k insulator (HK), metal gate (MG), non-uniform doping, [8] [9] [10] [11] [12] [13] has been suggested and utilised in device design. But, to maintain suitable electrostatic gate control over channel these innovations were not sufficient and many non-planer device architectures like Dual gate, Pi-gate, Omega Gate, FinFET/Tri-Gate were also proposed and investigated [14] [15] [16] [17]. But due to its



compatibility with semiconductor processing FinFET was the most successful [18]. FinFET was first introduced by Intel at the 22nm node and since then FinFET has become the most dominating technology. But with continued scaling trend, Fin structure also suffers. As channel doping engineering has serious drawbacks for small devices of current generation [19] [20], an architectural change is apparently one of the promising solutions.

Due to symmetry, Gate All Around (GAA) structure is theoretically the most suitable configuration from the gate electrostatic control point of view. In GAA FETs the insulating oxide and gate electrode both wrap around the channel. In this paper, we investigated the performance of GAAFET with the help of Silvaco TCAD tool. By changing various design parameters, a number of iterative simulations were performed, and effects of each parameter on device performance were observed. As expected the simulation shows that GAAFET with its four gates delivers much better gate electrostatic control over the channel. Even at 10nm and beyond, in GAAFET the SCEs are minimized and are fairly within acceptable limits. The ON to OFF current ratio of the device was also found excellent, making it power efficient and thus a solid option for portable devices. GAAFET's performance is further enhanced by minimizing corner effects i.e. by cylindrical channel.

## II. DEVICE PHYSICS

Following the trend of shrinking device dimensions, we have reached up to/beyond sub-deca nm feature size. At this size, the quantum mechanics became dominant over classical mechanics. It became difficult to control these devices, and Quantum corrections must be considered for accurately simulating and modeling the behaviour of such devices. In current work, quantum effects were considered by selecting appropriate models and their calibrated parameters were used. All simulations were performed using ATLAS device simulator tool of Silvaco TCAD. Bohm Quantum Potential model (BQP), Energy balanced model for electrons (HCTE.EL), and Field dependent mobility model (FLDMOB) were used in all simulations to get accurate results. Fermi-Dirac distribution instead of Boltzmann distribution was used for thermal equilibrium of carriers for initial guess. The physical device models used in the simulation are discussed below.

### 2.1 Bohm Quantum Potential Model

Quantum Potential models are originated from the hydrodynamic formulation of the quantum mechanics. The concept of Quantum potential was first introduced by de Broglie and Madelung [21]. Later Bohm further developed this model [22] [23]. In these models, the wave function of particle is written in terms of its amplitude and phase. These are then substituted back into the Schrodinger's equation to derive the following coupled equations of motion for density (1) and phase (2).

$$\frac{\partial \rho(\mathbf{r}, t)}{\partial t} + \nabla \cdot \left( \rho(\mathbf{r}, t) \frac{1}{m} \nabla S(\mathbf{r}, t) \right) = 0 \quad (1)$$

$$\frac{-\partial S(\mathbf{r}, t)}{\partial t} = \frac{1}{2m} [\nabla S(\mathbf{r}, t)]^2 + V(\mathbf{r}, t) + Q(\rho, \mathbf{r}, t) \quad (2)$$

Where,  $\rho(\mathbf{r}, t) = R^2(\mathbf{r}, t)$  is the probability density, Q is the Bohm Quantum Potential (3), V is potential term from Schrodinger equation and S is the solution of Hamiltonian-Jacobian equation [22]. Equation 1 has the form of continuity equation. Equation 1 and equation 2 are derived from Madelung transformation of the Schrodinger equation. These equations have the form of classical hydrodynamic equations with an additional potential

derived by Bohm's interpretation of Quantum mechanics and is known as Bohm Quantum Potential (BQP). BQP model used in our simulation was developed for Silvaco by the University of Pisa and has two advantages over density gradient method. First, it has better convergence properties in many situations. Second, it can be calibrated against results from the Schrodinger-Poisson equation under conditions of negligible current flow. BQP in ATLAS takes the following form[26]:

$$Q = \frac{-\hbar^2 \gamma \nabla \cdot (M^{-1} \nabla (n^\alpha))}{2 n^\alpha} \quad (3)$$

Where,  $\alpha$  and  $\gamma$  are two fitting parameters,  $M^{-1}$  is the inverse effective mass tensor and  $n$  is the electron (or hole) density. BQP method can also be used for the Energy balance and hydrodynamic models, where the semi-classical potential is modified by the quantum potential.

## 2.2 Energy Balance Transport Model

Simple Drift-Diffusion transport model has the limitation of not introducing the energy (carrier temperature) as an independent variable which makes it less accurate for deep submicron devices and too high gradients. So, for these devices, a higher order solution of general Boltzmann's Transport Equations (BTE) is required. Energy Balance Transport Model is a higher order solution to the general Boltzmann Transport Equation and consists of an additional coupling of the current density to the carrier temperature (or energy) model by introducing two new independent variables  $T_n$  and  $T_p$ , the carrier temperature for electrons and holes. The current density expressions from the drift-diffusion model are modified to include this additional physical relationship. The energy balance equations consist of an energy balance equation with the associated equations for current density and energy flux. For electrons, the Energy Balance Transport Model consists of [24]:

$$\text{div } S_n = \frac{1}{q} J_n E - W_n - \frac{3k}{2} \cdot \frac{\partial}{\partial t} (\lambda_n^* n T_n) \quad (4)$$

$$J_n = q D_n \nabla n - q \mu_n n \nabla \psi + q n D_n^T \nabla T_n \quad (5)$$

$$S_n = -K_n \nabla T_n - \left( \frac{k \delta_n}{q} \right) J_n T_n \quad (6)$$

Where  $T_n$  represent the electron temperatures,  $J_n$  is current density (5),  $S_n$  is the flux of energy (6),  $\mu_n$  is the electron mobilities,  $D_n$  is thermal diffusivity for electrons,  $W_n$  is the energy density loss rate for electrons, and  $K_n$  is the thermal conductivities of electrons.

## III. DEVICE SIMULATION

In the current work, device structures were made with DEVEDIT3d and simulated with ATLAS device simulator of Silvaco TCAD. In BQP model,  $\alpha$  and  $\gamma$  parameters were set to 0.3 and 1.4 resp. for calibration against Schrodinger-Poisson solver to set isotropic effective masses of Silicon to  $0.7 m_0$ . For solutions BLOCK iterative method was used, GUMMEL was used for initial guess, NEWTON RICHARDSON was used to speed up the calculations in iterations.

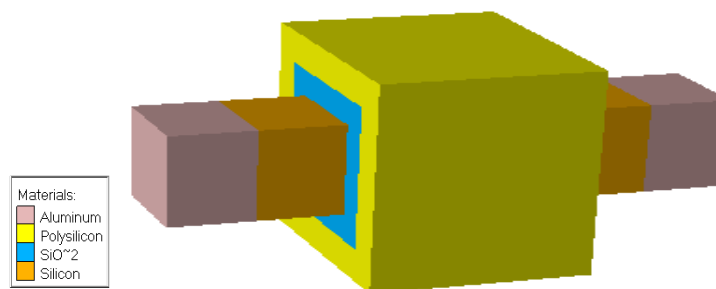


**Fig. 1: Gate All Around Field Effect Transistor**

Fig.1 shows the bird's eye view of the device structure simulated. The device is n-channel with SOI substrate. Poly-silicon was used as gate material, and Silicon dioxide ( $\text{SiO}_2$ ) was used as the insulating dielectric material. Other parameters are as follows: Gate length ( $L_g$ )=10nm, height ( $H$ ) = 7nm, width ( $W$ )=7nm, Oxide thickness ( $T$ )=2nm. Source and Drain doping= $1e^{19}$ atoms/cm<sup>3</sup> and doping profile set to Gaussian with Z roll-off of 0.5nm, Channel doping= $1e^{14}$  atoms/cm<sup>3</sup>. These values are taken as standard and are same throughout the paper unless mentioned.

#### IV. RESULTS AND DISCUSSION

Fig.2 shows the transfer characteristics of GAAFET device. These transfer characteristics were obtained at fixed Drain voltages ( $V_d$ ) of 0.05V and 0.5V. At each ( $V_d$ ), the Gate voltage ( $V_g$ ) was swiped from 0 to 0.8V. Drain current is plotted along Y-axis in  $\log_{10}(I_d)$  and Gate voltage along the X axis in Volts.

Output characteristics of GAAFET are plotted in Fig. 3. Three plots of  $I_d$  (along Y axis in Amperes) vs.  $V_d$  (along the X axis in Volts) are plotted at Gate bias of 0.45V, 0.55V, and 0.60V respectively. At each Gate bias ( $V_g$ ) Drain voltage ( $V_d$ ) was varied from 0 to 0.75V.

Detailed results of GAAFET simulation are summarized in **Table I**. Threshold voltage ( $V_{th}$ ) was calculated from the Transfer characteristics curve at a fixed drain current of  $0.3e^{-7}$ A [25]. **Beta** is the gain and **Theta** is Level-3 mobility roll off for SPICE simulation. Sub-threshold swing (**SS**) is in mV/decade. **DIBL** was defined as the difference in threshold voltage when drain voltage varied from 50mV to 0.5V.  $I_{ON}/I_{OFF}$  ratio was determined by extracting minimum and maximum current from the  $I_d$  vs.  $V_g$  curve.

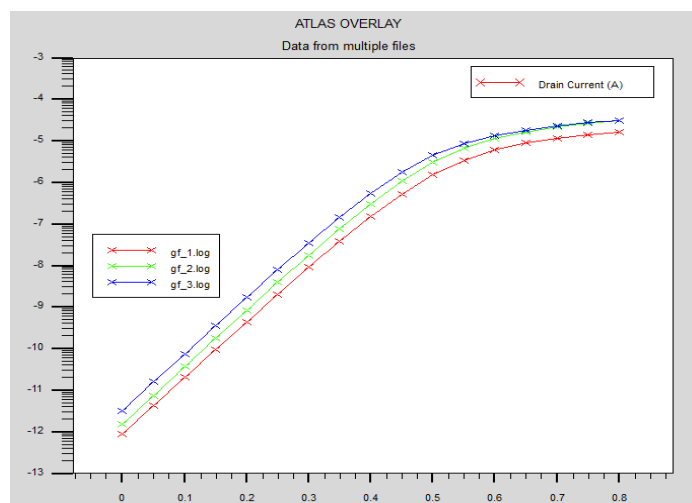


**Fig. 2: Transfer characteristics of GAAFET**

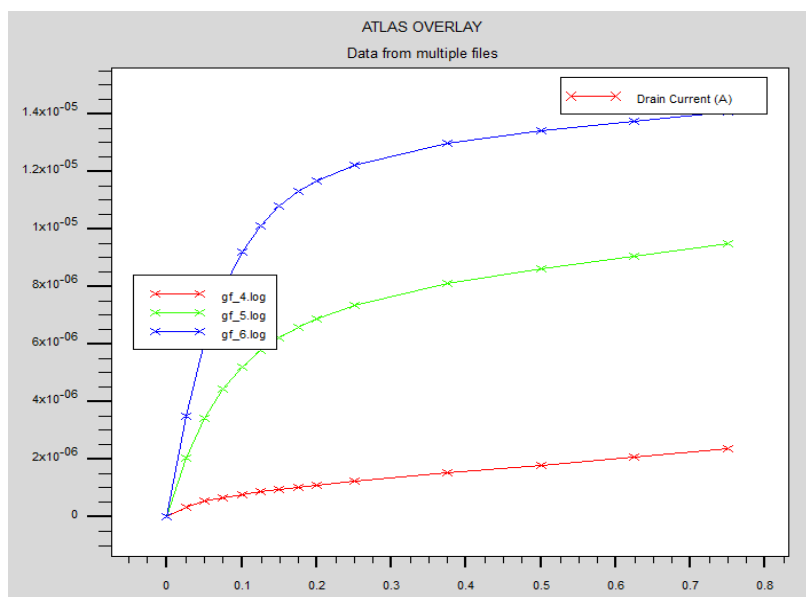


Fig. 3 Output characteristics of GAAFET

Table I: Extracted Results from GAAFET Simulation

Parameter Name	Vg=0.02V	Vg=0.1V	Vg=0.5V
V <sub>th</sub>	0.420	0.398	0.368
Beta	0.00116	0.00051	0.0019
Theta	0.83	0.84	0.77
SS	0.0735	0.0726	0.0722

I<sub>ON</sub> to I<sub>OFF</sub> ratio of GAAFET was found 1.9e<sup>7</sup>, which is excellent considering the small dimensions of the device. DIBL of GAAFET was calculated 113mV/V, which is within acceptable limits for a 10nm channel device. The variation of SS and DIBL with oxide thickness is shown in Fig. 4 and Fig. 5 respectively. As seen SS decreased from 85mV/V to 73mV/V when gate oxide thickness was reduced from 3nm to 1nm and DIBL decreased from 159mV/dec to 71mV/dec when gate oxide thickness was reduced from 3nm to 1nm.

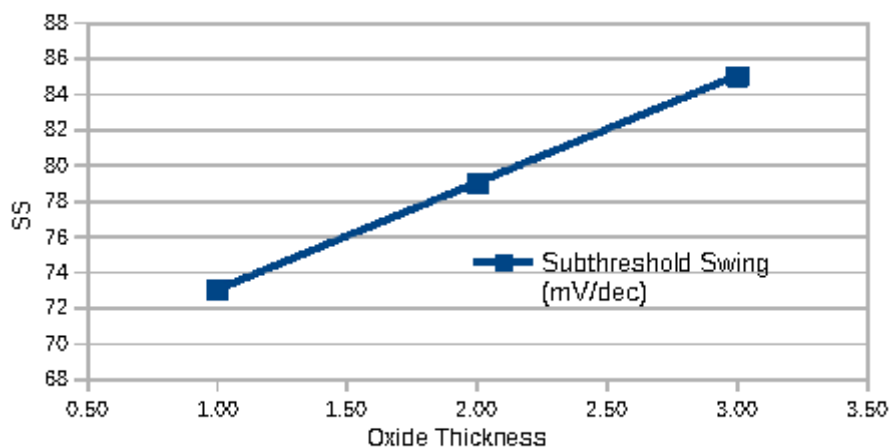
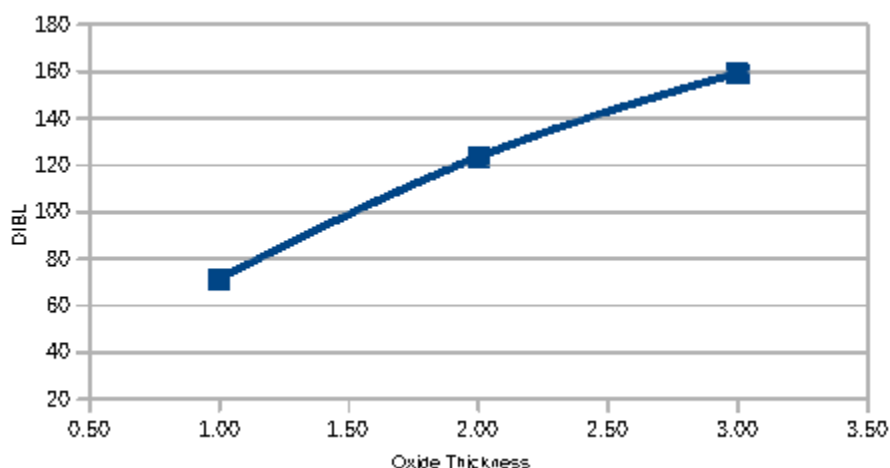
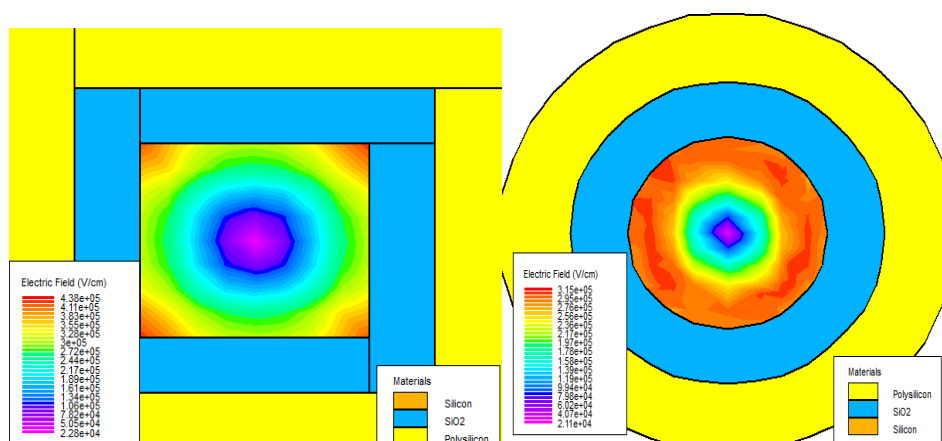


Fig. 4: SS versus Oxide thickness



**Fig. 5: DIBL versus Oxide thickness**

GAA MOSFETs generally suffer from corner effects. As shown in Fig. 6, the large electric field gathers around the edges of each channel in square GAA structure. The gate electrodes cannot sharply control the channels. This may cause short-channel effects. To observe the performance of corner effect free device the shape of GAA structure was changed to ideal cylindrical GAA structure and simulation was performed again.



**Fig. 6: Corner effects in square channel GAAFET**

The diameter of the channel was kept 7nm equal to the channel height and width of square channel GAAFET, oxide thickness was set to 2nm. The structure of ideal cylindrical channel GAAFET is shown in Fig. 7.

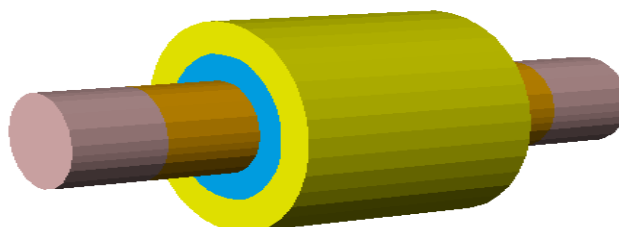


**Fig. 7: Ideal cylindrical channel GAAFET**

Due to its symmetrical nature, the cylindrical shape of the gate and channel eliminate the corner effects. The electric field as shown in the Fig. 6, is uniformly spanned in the circular rings within the channel. Cylindrical

channel shape provides better gate coupling and as expected the overall performance of the GAAFET was improved. The comparative results of simulations are summarized in Table II. In square channel GAAFETs the electric field near the corners of the channel was undesirably high which was resulting into high off current but in cylindrical channel device the off current was significantly reduced due to the strong and symmetrical electrostatic gate control over the channel which also improved the  $I_{on}/I_{off}$  ratio of the device. The relatively low saturation current in cylindrical channel GAAFET is justifiable by the fact that relative cross-section area of a 7nm diametric cylinder is small considering square of 7nm by 7nm. Also, these  $I_{dss}$  values are extracted at  $V_g=0.60V$ , and there is a difference in  $V_{TH}$  of both devices. The SCEs were also remarkably reduced in cylindrical GAAFET. DIBL and SS were found 78mV/dec and 71mV/V in Cylindrical GAAFET which were 113mV/dec and 73mV/V respectively in square channel GAAFET.

**Table II. Extracted Result of Square and cylindrical channel GAAFET Simulations**

Parameter Name	Square Channel GAAFET	Cylindrical Channel GAAFET
$I_{dss}$	$1.72e^{-5}$	$8.77e^{-6}$
$V_{TH}$	0.42	0.45
Beta	0.00116	0.00091
Theta	0.82	0.74
SS	0.073	0.071
DIBL	0.113	0.078
$I_{on}/I_{off}$	$1.8e^7$	$6.4e^7$

Fig. 8 shows the channel inversion in the square channel and cylindrical channel GAAFETs. It is seen that in the cylindrical channel device very strong and symmetrical volume inversion is achieved compared to square channel device.

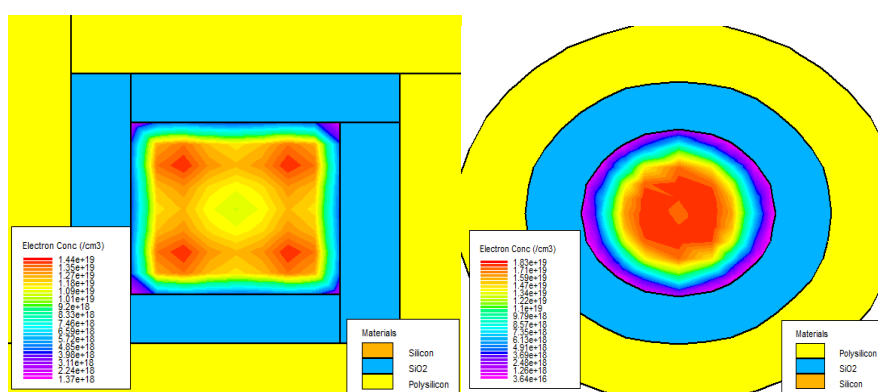


**Fig. 8: Channel inversion in the square channel and cylindrical channel GAAFETs; cylindrical channel GAAFET has more symmetrical and strong volume inversion.**

**VI. CONCLUSION**

The 3D simulation performed shows that even in deep sub-micron regime GAA structure has very good performance. The effect of the additional gate in GAA structure accounts for the enhanced performance of the device by providing better gate control over the channel. As seen from DIBL and SS parameters, GAAFET is robust to Short Channel Effects and can replace the Fin structure in future nodes. The ON to OFF current ratio of the cylindrical channel GAAFET is approximately five times better than that of the square channel GAAFET which proves that the cylindrical shape of the channel can further improve the performance of GAAFET making it ideal GAA structure from a performance point of view and for power efficient portable devices.

**VI. ACKNOWLEDGEMENT**

We are grateful to Department of Electronic Science for providing access to Silvaco TCAD tool in VLSI Design Laboratory.

**REFERENCES**

- [1] Moore, Gordon E. "Cramming more components onto integrated circuits, Reprinted from Electronics, 38(8), April 19, 1965, pp. 114 ff." IEEE Solid-State Circuits Society Newsletter 20(3),2006, 33-35.
- [2] Van Zeghbroeck, Bart, Principles of semiconductor devices, (Colorado University,2004).
- [3] Rusu S. Trends and scaling in VLSI technology scaling towards 100nm (Invited Paper), European Solid-State Circuits Conference (ESSCIRC), 2001.
- [4] N. G. Tarr, D. J. Walkey, M. B. ROWLANDSON, S. B. Hewitt, and T. W. McElwee Short-channel effects on MOSFET subthreshold swing, Solid State Electronics 38(3), pp. 697-701. 1995.
- [5] Y. Taur, L. H. Wann, and D. J. Frank, 25 nm CMOS design considerations, IEDM Tech. Dig., 1998, pp. 789-792.
- [6] Y. Taur, D. A. Buchanan, W. Chen, D. J. Frank, K. E. Ismail, S.-H. Lo, G.A. Sai-Halasz, R. G. Viswanathan, H.-J. C. Wann, S. J. Wind, and H.-S.P. Wong, "CMOS scaling into the nanometer regime," Proc. IEEE, 85(4), 1997, 486-504.
- [7] Y. Taur, "CMOS scaling beyond 0.1μm: how far can it go?" in Proc. Symp. VLSI Technology, 1999, 6-9.
- [8] Thompson, S. E., Armstrong, M., Auth, C., Alavi, M., Buehler, M., Chau, R., ... & Jan, C. H., A 90-nm logic technology featuring strained-silicon. IEEE Transactions on Electron Devices, 51(11),2004, 1790-1797.
- [9] Khakifirooz A, Cheng K, Nagumo T, Loubet N, Adam T, Reznicek A, Kuss J, Shahrjerdi D, Sreenivasan R, Ponoth S, He H. "Strain engineered extremely thin SOI (ETSOI) for high-performance CMOS. "In VLSI Technology (VLSIT), 2012 Symposium, IEEE, 2012, 117-118
- [10] Choi, Yang-Kyu, Kazuya Asano, Nick Lindert, Vivek Subramanian, Tsu-Jae King, Jeffrey Bokor, and Chenming Hu. "Ultra-thin-body SOI MOSFET for Deep-sub-tenth Micron era." In Electron Devices Meeting, 1999. IEDM'99. Technical Digest. International, IEEE, 1999, 919-921.
- [11] Schepis, D.J., Assaderaghi, F., Yee, D.S., Rausch, W., Bolam, R.J., Ajmera, A.C., Leobandung, E., Kulkarni, S.B., Flaker, R., Sadana, D. and Hovel, H.J., 1997, December. A 0.25μm CMOS SOI technology and

- its application to 4 Mb SRAM. In Electron Devices Meeting, IEDM'97. Technical Digest., International1997,587-590
- [12] Mistry, K., Allen, C., Auth, C., Beattie, B., Bergstrom, D., Bost & Choi, C. H., A 45nm logic technology with high- $k$  metal gate transistors, strained silicon, 9 Cu interconnect layers, 193nm dry patterning, and 100% Pb-free packaging, IEEE International2007, 247-250.
- [13] Henson, K., H. Bu, M. H. Na, Y. Liang, U. Kwon, S. Krishnan, J. Schaeffer, Gate length scaling and high drive currents enabled for high-performance SOI technology using high- $\kappa$ /metal gate, In Electron Devices Meeting, IEEE International, 2008, 1-4.
- [14] K. Suzuki, T. Tanaka, Y. Tasaka, H. Horie, and Y. Arimoto, Scaling theory for double-gate SOI MOSFETs, IEEE Trans. Electron Devices, 40, 1993, 2326–2329.
- [15] H.-S. P. Wong, D. J. Frank, Y. Taur, and J. M. C. Stork, Design and performance considerations for sub-0.1 $\mu$ m double-gate SOI MOSFETs, IEDM Tech. Digest., 1994, 747–750.
- [16] Choi, Yang-Kyu, Nick Lindert, Peiqi Xuan, Stephen Tang, Daewon Ha, Erik Anderson, Tsu-Jae King, Jeffrey Bokor, and Chenming Hu., Sub-20 nm CMOS FinFET technologies, In Electron Devices Meeting, Technical Digest. International, 2001, 19-1.
- [17] Doyle, B. S., S. Datta, M. Doczy, S. Harelund, B. Jin, J. Kavalieros, T. Linton, A. Murthy, R. Rios, and R. Chau., High performance fully-depleted tri-gate CMOS transistors, IEEE Electron Device, 24(4), 2003, 263-265.
- [18] D. Hisamoto, W.-C. Lee, J. Kedzierski, H. Takeuchi, K. Asano, C. Kuo, E. Anderson, T.-J. King, J. Bokor, and C. Hu, FinFET-a self-aligned double-gate MOSFET Scalable to 20 nm, IEEE Trans. Electron Devices, 47(12), 2000, 2320–2325.
- [19] K.J. Kuhn, Moore's Law past 32nm: Future Challenges in Device Scaling, Solid State Devices and Materials conference, Plenary, 2009.
- [20] Bin Yu, Leland Chang, S. Ahmed, Haihong Wang, S. Bell, Chih-Yuh Yang, C. Tabery, Chau Ho, Qi Xiang, Tsu-Jae King, J. Bokor, Chenming Hu, Ming-Ren Lin, D. Kyser, FinFET scaling to 10 nm gate length, Technical Digest of IEDM, 2002, 251.
- [21] Vasileska, Dragica, Stephen M. Goodnick, and Gerhard Klimeck. Computational Electronics: Semiclassical and Quantum Device Modeling and Simulation. CRC Press, 2016.
- [22] Bohm, David, A suggested interpretation of the quantum theory in terms of "hidden" variables. I, Physical Review 85(2), 1952, 166.
- [23] Bohm, David, A suggested interpretation of the quantum theory in terms of "hidden" variables. II, Physical Review 85(2), 1952, 180.
- [24] Iannaccone, Giuseppe, Gilberto Curatola, and Gianluca Fiori, Effective Bohm Quantum Potential for device simulators based on drift diffusion and energy transport, In Simulation of Semiconductor Processes and Devices, 2004, 275-278.
- [25] Ortiz-Conde, Adelmo, FJ Garcia Sánchez, Juin J. Liou, Antonio Cerdeira, Magali Estrada, and Y. Yue. "A review of recent MOSFET threshold voltage extraction methods." Microelectronics Reliability 42(4), 2002, 583-596.